

Pairing Interaction in N=Z Nuclei with Half-filled High- j Shell

A. Juodagalvis*

Mathematical Physics Division, Lund Institute of Technology,
S-22100 Lund, Sweden

Abstract

The role of $L=0$ pairing interactions (both $T=0$ and $T=1$) in three selected bands with the total isospin $T_{\text{tot}}=0$ in ^{22}Na , ^{48}Cr and ^{90}Rh nuclei is discussed in the spherical shell model. These bands were selected requiring termination in a most unfavourable way. The investigated effects coming from pairing interactions include the change of nuclear wavefunction, quadrupole properties and state energy. To follow the gradual change of nuclear properties, the investigation is performed in a perturbative approach by defining the Hamiltonian with a variable content of the pairing interaction. It is shown that the pairing interaction does not affect the quadrupole properties, if the energy distance to other close lying states is large. The calculated pairing energy is shown to have a similar spin dependence in these three bands. In addition, the influence of the model space as well as of the residual interaction on the derived pairing energy is discussed.

Key words: Shell model; Pairing energy; Schematic pairing interaction; Band termination; Electromagnetic properties; N=Z nuclei; ^{22}Na ; ^{48}Cr ; ^{90}Rh .

PACS: 21.10.-k, 21.10.Ky, 21.60.Cs

1 Introduction

The pairing force plays an important role for nuclear properties like binding energy, deformation, moment of inertia. It is a long standing question what is the quantitative role of the isoscalar ($T=0$) and isovector ($T=1$) pairing interactions. Their competition may be observed in the double-odd N=Z nuclei, where the lowest states with the total isospin $T_{\text{tot}}=0$ and 1 have very similar binding energy, and the transition from the $T_{\text{tot}}=0$ to $T_{\text{tot}}=1$ ground state, as the mass number increases, is seen. This phenomenon has recently regained attention, see e.g. [1] and references herein.

To investigate the role of the pairing interactions, many attempts were made to incorporate those correlations in the single-particle models like Hartree-Fock (HF) approximation (see e.g. [2, 3, 4, 5]). In the HF approach, the pairing correlations should be added. A different situation occurs in the shell model which takes into account the residual interaction completely. Here the pairing force is a part of the full interaction, and in principle it cannot be separated from the latter. It is known that the shell model Hamiltonian,

*e-mail: andriusj@matfys.lth.se

consisting of the single particle term and the $T=1$ pairing and quadrupole interactions [6], gives a reasonable description of nuclear properties. However, a question whether this is a sufficient minimal shell model Hamiltonian appeared again, when the theoretical background for strengths of pairing and quadrupole forces was reconsidered and it was shown that a schematic $T=0$ pairing is also an important part of the realistic interaction [7]. The interest was also stimulated by the availability of advanced shell model calculations (see e.g. [1, 8]) as well as by new experimental data available (e.g. [9, 10]).

This paper discusses the role of a schematic $L=0$ pairing. The two-particle states with spin S and isospin T equal to $ST=01$ or 10 are the ones favoured by Wigner's $SU(4)$ classification. Those states are also among the few lowest eigenvalues of the multipole part of a realistic Hamiltonian [7]. The real nuclear interaction breaks $SU(4)$ symmetry (e.g. by spin-dependence). However, it is not completely destroyed, and its presence shows up most clearly in the lighter nuclei through selection rules for β -decay.

The influence of the isoscalar and isovector $L=0$ pairing components of the effective interaction has been discussed for the nuclei in the middle of pf -shell [1, 8, 11]. The present paper refers to three $N=Z$ nuclei having half-filled high- j shell. These three selected nuclei (^{22}Na , ^{48}Cr and ^{90}Rh) are of particular interest. First of all, since protons and neutrons are occupying same shells, the neutron-proton interaction plays an important role. Another interesting feature is a rotational behaviour of the bands that terminate at spin $I_m=(p+1)^2\hbar$ (p is the principle quantum number of the harmonic oscillator shell). Those bands show backbending in the spin region (I_m-4, I_m-2). They terminate in a spherical state, since all components of the high- j shell orbits having positive angular momentum projection are occupied. In addition, they terminate in a “most unfavoured” way [12], since last two transitions before the termination involve breaking and alignment of two $T=1$ pairs (one neutron pair and one proton pair). Besides these three nuclei, such a band termination may occur in other nuclei (for example, an excited positive parity band in ^{47}Cr , having one hole in the sd -shell), but those bands would lie at higher excitation energy.

The most unfavoured band termination was the criterion to select particular bands in these three nuclei. These bands have the total isospin $T_{\text{tot}}=0$. The role of pairing interactions was investigated using the shell model. For two nuclei, ^{22}Na and ^{48}Cr , experimental data exists. But no data is available for ^{90}Rh , thus we have to rely on the ability of the chosen interactions to describe properties of the neighbouring nuclei. The aim of this paper is to show that the selected bands have some features in common, and that the $L=0$ pairing interactions change the properties of the bands in a similar way. The pairing influence to the nuclear wavefunction and quadrupole properties is also discussed.

The paper is organized in the following way. Computational details and comparison with experimental data are both discussed in section 2. Similarities in the selected bands as well as the predicted properties of the selected band in ^{90}Rh are also discussed in a greater detail there. At the end of the section, evaluation procedure of the role of pairing interaction is explained. The results are discussed in section 3. It is shown that the $L=0$ pairing interaction affects the behaviour of the selected bands in a similar way. And finally, conclusions are drawn in section 4.

2 Description of the approach

This section discusses three selected bands in a greater detail (subsection 2.1). Then computational details and comparison with experimental data are given (subsection 2.2).

Finally, an approach to extract the role of pairing interaction is explained (subsection 2.3). The obtained results are discussed later in section 3.

2.1 Bands having most unfavoured termination

Among the $N=Z$ nuclei, there is a special class of nuclei having exactly half-filled high- j shell. A peculiarity in these nuclei is that it costs more energy to construct the state, where all the valence particles are aligned in this high- j shell giving maximum spin $I_m=(p+1)^2$ (where p is the principle quantum number), than a rotational trend would suggest [12]. This effect comes mostly from $JT=01$ pairing interaction. It is interesting to see that there are similarities among the bands also in the spin dependence of the content of pairing energy.

In this paper, three $N=Z$ nuclei are discussed, namely, ^{22}Na , having 6 valence particles (3 protons and 3 neutrons) in the $d_{5/2}$, ^{48}Cr , having 8 particles in $f_{7/2}$, and ^{90}Rh , having 10 particles in $g_{9/2}$ shell, when the single-particle level ordering from a harmonic oscillator potential with ℓ^2 and $\ell \cdot s$ terms is assumed. In the single- j shell model with the $JT=01$ pairing interaction only, bands leading to the maximum spin state behave in a similar way (see fig.1a). Let I_m is the spin of a completely aligned state (which should be spherical since all orbits with positive \vec{j} projections are occupied): $I_m=9\hbar$ for ^{22}Na , $16\hbar$ for ^{48}Cr , and $25\hbar$ for ^{90}Rh . Let us discuss only the lowest states at spins I_m-2k where k is an integer number. These states have the total isospin $T_{\text{tot}}=0$. The state with spin I_m-2 would be a linear combination of states where one pair of identical particles is coupled to angular momentum 0, and the spin is obtained from the remaining unpaired particles. Similarly, the I_m-4 state would have two pairs of particles (one neutron pair and one proton pair) coupled to angular momentum 0. For ^{22}Na , that is the maximum spin state produced by two odd particles (5^+ , bandhead $K^\pi=3^+$). Since there is no change in the pairing energy when going from I_m-4 to I_m-6 state, the I_m-4 state may be somewhat irregular in the real energy spectrum. In the discussed cases there is a backbending in ^{48}Cr and ^{90}Rh , but in general the change of the moment of inertia may be less pronounced. The state with spin I_m-10 (having 10 units of $JT=01$ pairing energy in a single- j model, see fig.1a) would be a linear combination of states where 6 particles contribute angular momentum zero: two pairs of one kind and one pair of the other kind of particles are all contributing angular momentum 0. Since at least 6 valence particles are not contributing to spin, the irregularity in the energy spectrum may be not seen unless this j -shell is dominating. The state I_m-16 would have 4 angular-momentum-zero pairs. This state is the ground state in ^{48}Cr , while in ^{90}Rh it is the maximum spin obtained from odd proton and neutron (9^+ , bandhead $K^\pi=5^+$).

There are more bands terminating in a most unfavourable way. One can think of lighter nuclei with half-filled high- j shell of harmonic oscillator major shells having principle quantum number $p=1$ or 0 (^8Be and ^2H , respectively), but there are very little states before the maximum spin state, thus no bands are formed. A more realistic examples are excited bands in nuclei close the three earlier mentioned nuclei. First example could be one-particle-one-hole (1p-1h) bands of unnatural parity in nuclei having mass number (A_m-1) (here A_m is the mass number of any of the three middle high- j shell nuclei). For example, an excited band in ^{21}Ne (or ^{21}Na), where one proton (neutron) is excited from the p - to sd -shell. This band would terminate at spin $I=9+j_h$, where j_h equals $1/2$ or $3/2$ depending on the position of the hole in p -shell. Other examples are ^{47}Cr (or ^{47}V) and ^{89}Ru (the band in ^{89}Rh is less likely to be observed, at least in the nearest future). One

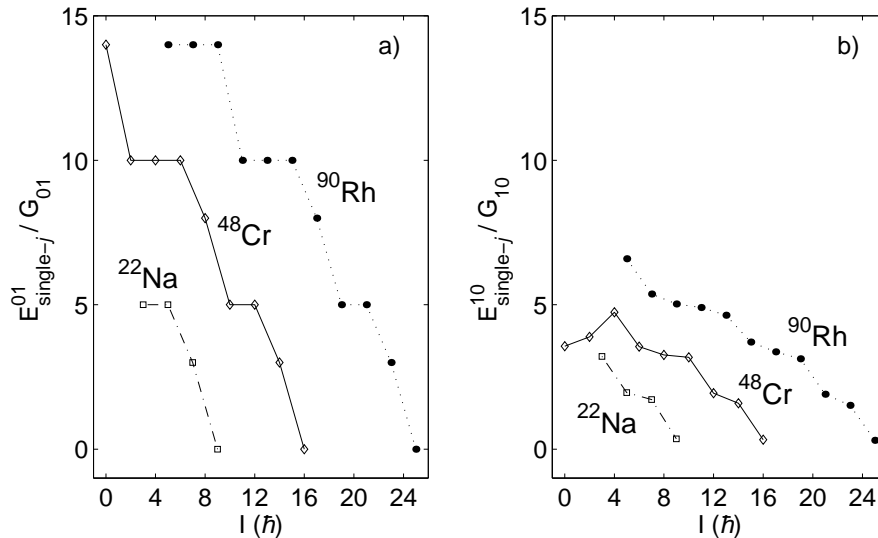


Figure 1: Spin dependence of the JT pairing energy in the lowest $T_{\text{tot}}=0$ states in the model space consisting of a high- j shell only. The $JT=01$ case is shown on the left, while $JT=10$ case is shown on the right. Formula for the $JT=01$ pairing energy, parameterized in terms of the total seniority and reduced isospin, is taken from [13].

can also think of bands based on 2p-2h excitation in (A_m-2) mass nuclei, and so on.

The most unfavoured band termination may also be encountered in cases when the last transition before the band termination involves alignment of a pair (coupled to angular-momentum-zero) that brings only $2\hbar$, and the relative difference of neutron and proton seniorities (i.e. the reduced isospin) decreases. In the cases discussed in this paper, the reduced isospin is zero at spin I_m-4 , then it increases at state I_m-2 and decreases again at the aligned state with the total angular momentum I_m .

The discussion of pairing features in a single- j shell is based on the fact that the high- j shell dominates in the cases discussed here, i.e. either it has the largest occupancy and/or its change has greater impact to the band properties. For example, shell occupancies in some states of ^{48}Cr are shown in fig.7 (occupancies in all yrast states of ^{48}Cr may be found in ref.[14]). The shell occupancies along the selected band in ^{90}Rh are shown in fig.4.

The role of $JT=01$ pairing interaction is well acknowledged. The seniority quantum number led to an additional classification of many-particle configurations. While the role of $JT=10$ pairing interaction is less pronounced: models without this interaction successfully describe nuclear properties, and there is no additional (and useful) classification in terms of $JT=10$ coupled pairs. Although in the realistic interactions $JT=10$ pairing is stronger than $JT=01$ [7]: the ratio of the strength parameters $G_{10}/G_{01}\approx 1.5$, see e.g. Table 1; the features of this pairing interaction in a single- j shell (see fig.1b) are less prominent in the calculated or observed spectrum. For example, the behaviour of $JT=10$ energy in a single- j model predicts an increased energy loss between states having spins I_m-6 and I_m-4 . In the observed spectra (fig.2) as well as in the full calculations (figs.2,3), there is a backbending between those states, i.e. the behaviour is opposite to the predicted from the $JT=10$ pairing energy spin-dependence in a single high- j shell. It may be noted, however, that the unequal energy spacing between states with spins I_m-4 , I_m-2 and I_m is predicted by $JT=10$ as well as by $JT=01$ pairing interaction.

One reason for the small relative importance of $JT=10$ pairing may be the fact, that the interaction matrix elements of $JT=10$ pairing are smaller than those of the $JT=01$:

for example, in the single- j case, the ratio of the matrix elements is $G_{10}/G_{01} (j+1)/(3j)$ which is less than 1 for $j > \frac{1}{2}$. The pairing energy would be larger if the high- j shell spin-orbit partner would be included in the model space, as discussed below in subsection 3.2.1. However, that does not change much the spin dependence of the pairing energy (see fig.14). Thus the main reason, why the $JT=10$ pairing interaction was not found being important, may be its smooth spin dependence (see fig.1b). Small irregularities suggested by fig.1b are likely to be found only in the cases when $JT=01$ pairing energy does not change. Another possibility could be the cases when $JT=01$ pairing is blocked, e.g. in the doubly-odd nuclei [11]. In subsection 3.2.2 it is discussed that the $JT=10$ pairing interaction may be responsible for the favouring of $I=7$ state in ^{90}Rh calculated using SSSV interaction.

The discussion above was referring to the pairing energy spin dependence along *one* band, and is continued in subsection 3.2.3. One may find a more general discussion about the relative importance of $JT=01$ and $JT=10$ pairing energies in the shell model framework in ref. [1].

2.2 Computational details and comparison with experiment

In present work, shell model calculations were performed using the computer code ANTOINE [15]. The residual interactions, used in the calculation, were: USD [16] interaction in the full sd -shell for ^{22}Na , KB3 [17] in the full pf -shell for ^{48}Cr , Gross and Frenkel interaction [18] (referred to as GF) as well as SLGT0 [19] in $p_{1/2}g_{9/2}$, and Sinatkas et al. [20] (referred to as SSSV) in $g_{9/2}p_{1/2}p_{3/2}$ for ^{90}Rh . Electromagnetic quadrupole properties were calculated using the effective charges $q_\pi=1.5e$ for protons and $q_\nu=0.5e$ for neutrons.

Fig. 2 presents a comparison of the calculated and experimental energies of the selected $T_{\text{tot}}=0$ states in ^{22}Na and ^{48}Cr : These are odd-spin members of the ground state band having $K^\pi=3^+$ in ^{22}Na (experimental data taken from [21]), and the ground state band having $K^\pi=0^+$ in ^{48}Cr (experimental data taken from [22]). As can be seen, the agreement between experimental data and calculated values is excellent. There is no experimental data available on ^{90}Rh . In fig.3 the calculated odd-spin members of the $K^\pi=5^+$ band in ^{90}Rh are shown. Those two figures (1 and 2) show, that after a rotational reference E_{rot} is subtracted, the bands tend to bend up close to the band termination (so-called “unfavoured band termination” [23]). In addition, the state I_m-4 deviates from a regular behaviour of the preceding states (not seen in ^{22}Na , since there is only one such state). The irregularity at spin I_m-10 , discussed in subsection 2.1 as being possible to occur, is not seen in ^{48}Cr and ^{90}Rh at $I=6$ and 15, respectively. The exceptions are GF and SLGT0 calculations of ^{90}Rh , where a very restrictive model space allows rather poor shell mixing. The calculated probability of a configuration, where all active particles are in the high- j shell producing spin I_m , is large: $>90\%$ for ^{48}Cr as well as ^{90}Rh (SLGT0 and SSSV calculation), 54% for ^{22}Na , and 62% for ^{90}Rh (GF).

Since there is no experimental data on ^{90}Rh available, only calculated states are shown in fig.3. Calculations were performed in the configuration spaces $(p_{1/2}g_{9/2})^{14}$ with GF and SLGT0 (cf.[19]) interactions, and $(g_{9/2}p_{1/2}p_{3/2})^{-10}$ using SSSV interaction. These three residual interactions predict that the ground state has spin $I=0$ and the total isospin $T_{\text{tot}}=1$, in agreement with the mass-dependence of the both spin and isospin in the ground state of doubly-odd nuclei [25]. The excitation energy of the lowest $T_{\text{tot}}=0$ states is predicted to be ~ 1.3 MeV. The SSSV interaction predicts almost spherical ground state of ^{90}Rh , with the deformation $\beta \approx 0.13$ (value estimated from $B(E2; 2_1^+ \rightarrow 0_1^+, T_{\text{tot}} = 1)$,

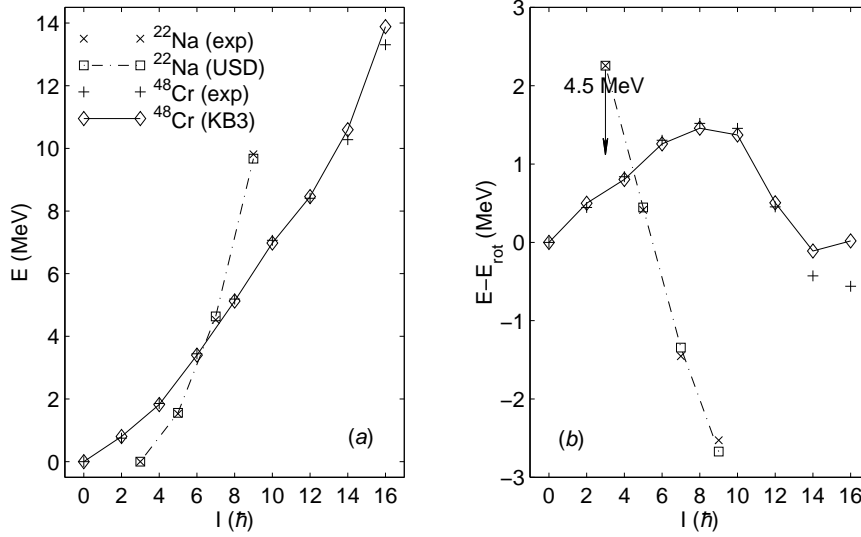


Figure 2: Energies of selected bands in ^{22}Na and ^{48}Cr . For the calculated states, the residual interaction is given in parentheses. Calculated spectra of ^{22}Na and ^{48}Cr were reported in refs. [16] and [24], respectively. Plot *a* shows excitation energies, and plot *b* shows the same energies but with a rotational reference, $E_{\text{rot}}=32.32A^{-5/3}I(I+1)$, subtracted. In the latter plot, 4.5 MeV was added to all energies in ^{22}Na to make the figure more compact, that is also indicated by an arrow.

assuming axially symmetric rotor model is valid). The interactions, however, predict slightly different behaviour of the band of interest. For example, the SSSV interaction favours $I^\pi=7^+$ state as compared to the 5^+ state. In addition, energies calculated in a more restricted model space (with the GF and SLGT0 interactions) are more irregular than those obtained using the SSSV interaction, see fig.3*b*. Like in ^{48}Cr case at spin $I_m-10=6^+$, there is no irregularity at spin $I_m-10=15^+$ in ^{90}Rh according to the SSSV calculation. That may be explained by the shell mixing (see occupation numbers in fig.4). The band terminates at spin $I_m=25^+$ in an almost spherical shape, with a half-filled $g_{9/2}$ shell. An exception is the GF calculation where the terminating state contains 62% probability of configuration $(p_{1/2}^2g_{9/2}^5)^2$ and 37% of $(p_{1/2}^1g_{9/2}^6)^2$, and the nucleus has an oblate shape. The band termination is also indicated by a decrease in $B(E2)$ values (see fig.5*a*). All three interactions suggest that the $K^\pi=5^+$ band in ^{90}Rh backbends at spin $I_m-6=19^+$. Backbending will be discussed after comparison of the calculated occupation numbers and $E2$ properties.

The calculated j -shell occupancies (average number divided by the maximum number of particles in the shell) in ^{90}Rh are shown in fig.4. To get particle occupancies in the SSSV calculation, the average number of holes was converted to the average number of particles. As can be seen from the figure, the $p_{1/2}$ shell is filled almost all the time (occupancy is greater than 90% for most spin values) in the GF as well as SLGT0 calculations, resulting in a half-filled $g_{9/2}$ shell for all band states (except for the spin I_m state in the GF calculation, as mentioned above). While in the SSSV calculation, this shell contains more than 10 particles (is more than half-filled) for spins $I < 21$. The mixing reduces for $I \geq 21$, when 6 particles aligned in the $g_{9/2}$ shell may contribute $21\hbar$. Note that an increase of the $f_{7/2}$ shell occupation by particles, approaching the aligned state $I_m=16$ in ^{48}Cr [14], corresponds to an increase of the $g_{9/2}$ shell occupation by holes as spin increases to $I_m=25$ in ^{90}Rh in the SSSV calculation.

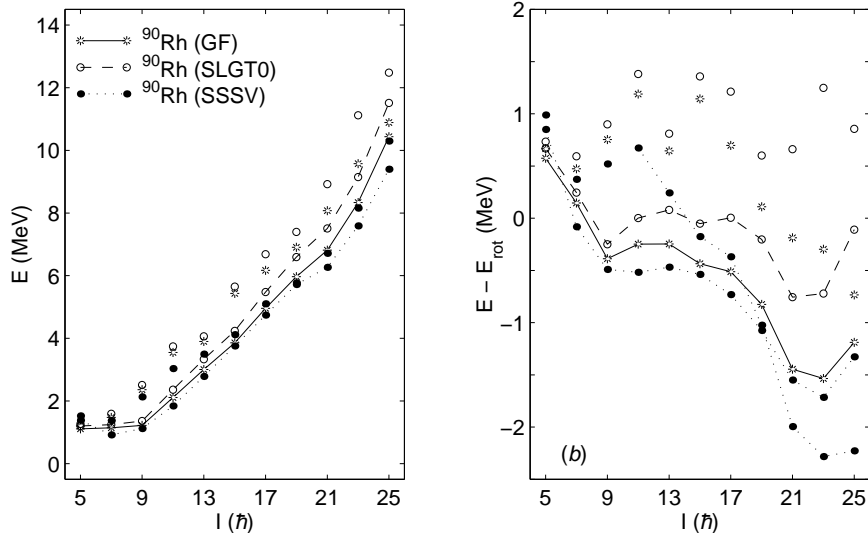


Figure 3: Energies of odd- I members of $K^\pi=5^+$, $T_{\text{tot}}=0$ band in ^{90}Rh calculated with GF, SLGT0 (cf.[19]) and SSSV interactions. For explanations see fig.2. Yrast states are connected by lines, while second excited states for each spin value are indicated by a corresponding symbol not connected by a line, except for the SSSV results shown in plot b , where the states forming bands (having large $E2$ transition strengths) are connected by dotted lines.

The calculated $E2$ transition strengths in ^{90}Rh are shown in fig.5a. The $B(E2)$ values calculated using SSSV interaction are larger than those obtained in GF or SLGT0 calculations, implying larger deformation and thus greater collectivity, as also seen from the energy plot with a rotational reference subtracted, fig.3b. Additional reason for smaller $E2$ transition strengths in more restricted calculations is that $p_{1/2}$ does not contribute, thus there is only contribution from the $g_{9/2}$ shell. In the case of half-filled j -shells, there is an additional suppression of the $E2$ transition strengths due to so-called “the center-of-the-shell selection rule” [26]: in a single- j configuration the spectroscopic moment vanishes, and the $E2$ transition can only take place between states differing in seniority by two units, if this j -shell is half-filled. Indeed, the occupancies (fig.4) show that the $g_{9/2}$ shell is almost always half-filled, $Q_{\text{spec}} \approx 0$, and $B(E2)$ are relatively small (fig.5) in GF as well as in SLGT0 calculation. The negative sign of Q_{spec} calculated with the SSSV interaction (fig.5b) suggests prolate deformation along the band.

All three calculations of ^{90}Rh predict a backbending at spin $I_m-6=19^+$, as would be expected from the discussion of band properties in a single- j shell assuming only $JT=01$ pairing interaction being important (subsection 2.1). In the SSSV case, the backbending may be explained in terms of a band-crossing. The bands are shown in fig.3b where the calculated states are connected if there is a strong stretched $E2$ transition between them. As can be seen from the figure, yrare band crosses yrast band (“ $K^\pi=5^+$ band”) between spins $I=19$ and 21. For the spins below $21\hbar$, the excited band has lower particle occupation of the $g_{9/2}$ shell (approximately 0.55) as compared to the yrast band value, ≈ 0.68 (fig.4). States $21_{1,2}^+$ have almost identical occupation numbers. For higher spins the $g_{9/2}$ shell occupation drops down to 0.5 in the yrast band, but equals 0.67 and 0.60 at states with spins 23_2 and 25_2 , respectively. The $B(E2)$ values along the band with a lower occupation of the $g_{9/2}$ shell are very similar to the GF and SLGT0 results (cf fig.5a), except for the transition $13_2^+ \rightarrow 11_2^+$ that is stronger, ~ 14.4 W.u. The Q_{spec} values

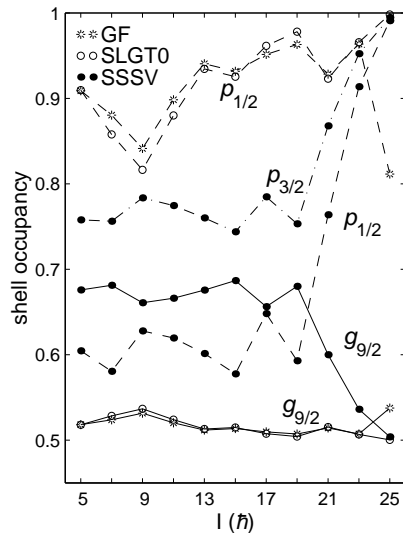


Figure 4: Calculated shell occupancies in $K=5^+$ band in ^{90}Rh . Three residual interactions were used: GF (marked by stars) as well as SLGT0 (open circles) in the configuration space $(p_{1/2}g_{9/2})^{14}$, and SSSV (filled circles) in $(g_{9/2}p_{1/2}p_{3/2})^{-10}$. The j -shell is indicated close to a corresponding line. In the SSSV case, the number of holes was converted to the number of particles in shells.

are approximately constant along this band, $-10 \text{ e}\cdot\text{fm}^2$, while at $I=21$ Q_{spec} decreases to $-38.0 \text{ e}\cdot\text{fm}^2$. The continuation of “ $K=5^+$ band” has larger intra-band $B(E2)$ values, than those calculated for the yrast states, except for the transition starting at spin 25_2^+ . The values are 1.4, 10.6 and 12.9 W.u. for transitions from state 25_2^+ to state 23_2^+ , from 23_2^+ to 21_2^+ , and from 21_2^+ to 19_1^+ , respectively. The spectroscopic quadrupole moment for the states $I=21_2-25_2$ is varying around the value of $-50 \text{ e}\cdot\text{fm}^2$.

The $B(E2)$ value calculated using SSSV interaction is reduced for the transition $I_i \rightarrow (I_i - 2)$, where $I_i = I_m - 4 = 21\hbar$. A straightforward explanation could be the fact that this transition connects two “rotational bands” having somewhat different structure, seen either in terms of the $g_{9/2}$ shell occupancy or the spectroscopic quadrupole moment. An alternative explanation could be the “center-of-the-shell” selection rule, mentioned above: the vanishing $E2$ transition would indicate purity of the half-filled single- j configuration [26]. In subsection 2.1 it was discussed that the seniorities of states $I_m - 6$ and $I_m - 4$ are equal, thus the conditions for the selection rule are favourable. However, the Q_{spec} does not vanish neither at 19_1^+ nor at 21_1^+ (see fig.5b), suggesting that the selection rule is not involved. While the structure of nuclear wavefunctions of those states is very different, and that is the reason for the reduced $B(E2)$ value.

A comparison of the predicted spin dependencies of the $B(E2)$ values in ^{90}Rh (fig.5) yields another question: whether the reduction of $B(E2)$ at $I_i = 21_1^+$ is a feature of the SSSV interaction. The more restricted calculations do not predict reduction. On the other hand, they do not predict bandcrossing as a reason for the backbending. A similar situation occurs in ^{48}Cr calculated using the modified surface-delta interaction [12] (MSDI) in the configuration space $(f_{7/2}p_{3/2})^8$, see fig.5a. This interaction, fitted for this nucleus, describes excitation energies of the yrast states in ^{48}Cr a bit better than the KB3 interaction does. The lowest bands predicted in ^{48}Cr by both KB3 and MSDI interactions are somewhat similar to those predicted in ^{90}Rh by the SSSV: In ^{48}Cr the yrast band continues above the backbending preserving the nuclear structure; however, the band,

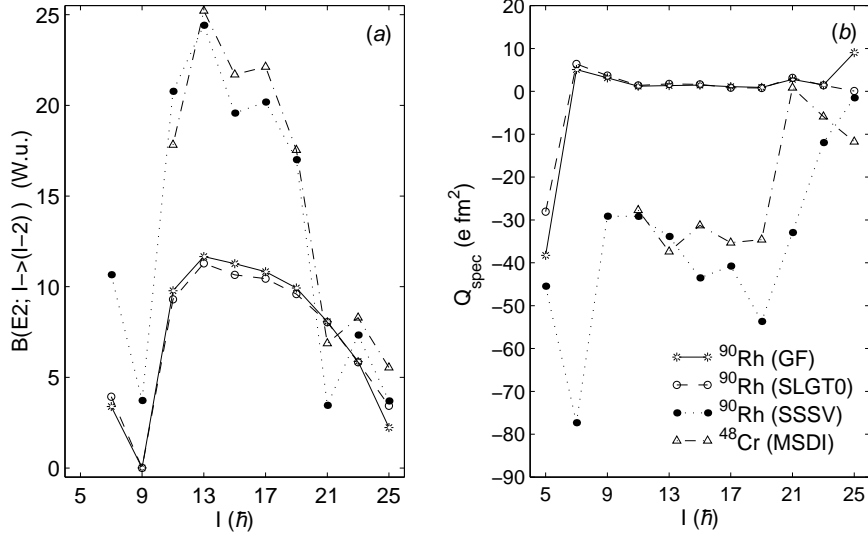


Figure 5: Calculated $E2$ properties along the $K\pi=5^+$ band in ^{90}Rh and the ground state band in ^{48}Cr : strengths of stretched $E2$ transitions, $B(E2)$, are shown on the left; and spectroscopic moments, Q_{spec} , are shown on the right. Values for ^{90}Rh were calculated using the GF (marked by stars), SLGT0 (open circles) and SSSV (filled circles) interactions. The modified surface-delta interaction (referred to as MSDI and marked by triangles) in the model space ($f_{7/2}p_{3/2}$) [12] was used for ^{48}Cr , and the spin values for ^{48}Cr are shifted by $9\hbar$.

terminating at spin $I_m=16^+$, cannot be traced back below the backbending. The $B(E2)$ values calculated in ^{48}Cr using MSDI are systematically smaller, most probably due to a restricted model space. Nevertheless there is a reduction of the $B(E2)$ value for the transition starting at spin $I_i=I_m-4=12$ in the MSDI calculation. (It is not clear why the Q_{spec} vanishes at spin $12\hbar$, see fig.5b. The selection rule would suggest, that it is an indication of a rather pure $(f_{7/2})^8$ configuration, however, the calculated probability of this configuration at this spin value is only 69%. But on the contrary to the selection rule prediction, the increasing probability of $(f_{7/2})^8$ is followed by the decrease of Q_{spec} for spins 14 and 16.) However, the relative decrease of $B(E2; 12_1^+ \rightarrow 10_1^+)$ was not observed [22]. This decrease is also not predicted by the KB3 [24]. Thus, having confronted the different predictions for the ^{90}Rh and ^{48}Cr nuclei, a conclusion may be drawn that only lifetime measurements or the calculation in a more extended model space may suggest a solution to the puzzle whether there is a decrease in $B(E2; I_i \rightarrow I_i - 2)$ values at $I_i=21$ in ^{90}Rh .

2.3 Estimation of the role of pairing interactions

The role of *normalized* $L=0$ pairing interactions [7] is discussed in present paper. Notations for the forces used in the latter reference are adopted. Thus \bar{P}_{01} (or simply 01 as an index, e.g. E_{01}) will stand for the normalized isovector $J=0$, $S=0$, $T=1$ pairing interaction, and \bar{P}_{10} (or 10) will stand for the normalized isoscalar $J=1$, $S=1$, $T=0$ pairing interaction. The pairing strength parameters are taken from eq.(C3) in ref.[7]. They are defined in terms of a constant multiplied by a scaling parameter, $\hbar\omega$: $\bar{G}_{01}=-0.32\hbar\omega$ and $\bar{G}_{10}=-0.51\hbar\omega$. An expression for $\hbar\omega$ is taken from [27], and the resulting strengths are given in Table 1.

Table 1: Strength parameters of normalized pairing interactions used in present paper

| Pairing type | ²² Na | ⁴⁸ Cr | ⁹⁰ Rh |
|------------------------------|------------------|------------------|------------------|
| $\bar{P}_{01}, \bar{G}_{01}$ | -3.80 | -3.19 | -2.68 |
| $\bar{P}_{10}, \bar{G}_{10}$ | -6.05 | -5.09 | -4.27 |

The pairing interaction influence (i) to the state energy, (ii) the nuclear wavefunction and (iii) quadrupole properties will be discussed. Investigation is performed in a perturbative way, by comparing results obtained with the full Hamiltonian and the Hamiltonians having reduced content of some pairing interaction (either \bar{P}_{01} or \bar{P}_{10}). It will be shown that in some cases, a competition between the pairing and the rest of the residual interaction may be seen. (Cf. discussion about the interplay between the quadrupole and the monopole parts of the Hamiltonian in ref.[28].)

The Hamiltonian without \bar{P}_{JT} pairing, $H_{JT}(0)$, is defined as a full Hamiltonian, H , from which the normalized pairing interaction, W_{JT} , has been subtracted (in a similar way KB3-P01 and KB3-P10 were defined in ref. [8], but the pairing interactions were not normalized. Note, however, that normalized and unnormalized forms are equivalent for a single major shell):

$$H_{JT}(0) = H - W_{JT}, \quad (1)$$

where $JT=01$ for the isovector (\bar{P}_{01}) and 10 for the isoscalar (\bar{P}_{10}) $L=0$ pairing interaction; and the meaning of 0 in parentheses will be seen later. To investigate the role of a JT pairing interaction in a perturbative way, let's define a Hamiltonian $H_{JT}(\lambda)$ that has some content of the pairing interaction indicated by a weight parameter λ ($0 \leq \lambda \leq 1$):

$$H_{JT}(\lambda) = H_{JT}(0) + \lambda W_{JT}. \quad (2)$$

Thus $H_{JT}(\lambda)$ ($\equiv H_{JT}$) is a linear interpolation between the Hamiltonian without pairing, $H_{JT}(0)$, and the full Hamiltonian, $H_{JT}(1)=H$. One can parameterize the eigenvalues of this Hamiltonian in the following way:

$$E_{JT}(\lambda) = E_{JT}(0) + \langle W_{JT} \rangle \lambda + \chi(\lambda), \quad (3)$$

where $E_{JT}(0)$ is an eigenvalue of the Hamiltonian without \bar{P}_{JT} pairing interaction, $E_{JT}(\lambda)$ is an eigenvalue of the Hamiltonian $H_{JT}(\lambda)$, $\langle W_{JT} \rangle$ is the expectation value of the normalized JT pairing interaction, and $\chi(\lambda)$ describes additional terms which are non-linear in λ . One can see that $\chi(0) \equiv 0$. If $\chi(\lambda)$ is set to 0, the equation (3) describes first-order perturbation to the energy $E_{JT}(0)$. The energies are calculated and parameterized for each spin value separately, i.e. the quantities defined by eq.(3) have additional index - spin I - which is omitted (thus the eigenvalues in full notation are $E_{JT}(\lambda; I)$). The expectation value of the pairing interaction, $\langle W_{JT} \rangle$, may be evaluated directly from the calculated nuclear wavefunction (cf. ref.[1]). However, it was not possible to perform such evaluation in present investigation.

An example of the H_{JT} eigenvalue spectrum dependence on the pairing interaction content is given in fig.6, where energies of the yrast states in ⁴⁸Cr calculated using the KB3 interaction are shown as a function of parameter λ . The case when \bar{P}_{01} interaction content is varied is shown on the left, while the \bar{P}_{10} case is shown on the right. The

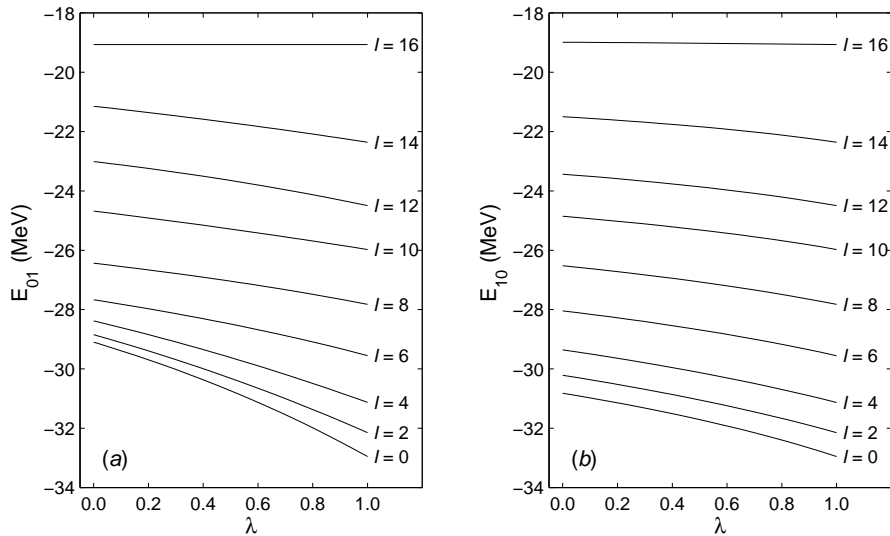


Figure 6: Calculated energies of yrast states in ^{48}Cr as a function of the \bar{P}_{JT} pairing interaction content. KB3 interaction is used. The spin is indicated by a number close to the corresponding line. Plot *a* (*b*) shows the case $JT=01$ (10).

meaning of parameters in eq.(3) may be seen from this figure: $\langle W_{JT} \rangle$ is the slope of the $E_{JT}(\lambda)$ line at $\lambda=0$, and $\chi(\lambda)$ is the deviation of $E_{JT}(\lambda)$ values from the linear behaviour ($E_{JT}(0) + \langle W_{JT} \rangle \lambda$). One can see that $|\chi(\lambda)|$ increases together with λ (the lines bend down), and that non-linear contributions are largest for lower spins. Since the slope of the $E_{JT}(\lambda)$ line is proportional to the average number of JT -coupled pairs, it is clearly seen that there are more such pairs in the nuclear wavefunction calculated with a Hamiltonian close to the full Hamiltonian. Which may be understood from the fact that pairing interactions increase the binding energy of a pair, thus pairing correlations are more favourable if pairing force is stronger, i.e. the pairing interaction content in the Hamiltonian is larger.

Lets define the pairing energy, ΔE_{JT} , which will show the increase in the binding energy of a state having spin I due to an addition of the JT pairing interaction:

$$\Delta E_{JT} \equiv E_{JT}(0) - E(1), \quad (4)$$

where $E(1)$ is the state energy calculated with the full Hamiltonian, and $E_{JT}(0)$ is the state energy calculated using the Hamiltonian without \bar{P}_{JT} pairing interaction; additional index - spin I - is omitted. The pairing energy will always be non-negative, since the pairing interactions are attractive, i.e. they increase binding.

A Hamiltonian may be considered as consisting of monopole and multipole parts [7], where the monopole part is responsible for the correct nuclear binding energies at the observed nuclear radii and for the single-particle behaviour, and the multipole (or residual) part describes collective properties and is responsible for configuration mixing. One may notice that the pairing interactions contribute to both parts: the changed content of the pairing interaction affects the monopole part due to the moved centroids of the total interaction, while the multipole part is affected because this interaction is responsible for correlations (only this part of a pairing interaction, that contributes to the multipole Hamiltonian, may be viewed as being responsible for pair correlations in the spherical mean-field sense). The strengths of pairing interactions were derived in ref.[7] from a monopole-free Hamiltonian. However, in present investigation it was not possible to make

exact separation of the pairing effects into monopole and multipole parts in a consistent way, thus only total effect is investigated. One term in the monopole part of the Hamiltonian, namely, the single-particle contribution, may be readily evaluated having j -shell occupation numbers. The single-particle term may be written as:

$$K^d = \sum_{\{j\}} n_j \varepsilon_j, \quad (5)$$

where ε_j is the single-particle (or single-hole) energy of a j -shell, and n_j is the average number of particles in the shell.

In a similar manner as the change of binding energies (the pairing energy) is defined in eq.(4), one can define the change of the single-particle contribution as an outcome of pairing interaction:

$$\Delta K_{JT}^d = K_{JT}^d(0) - K^d(1), \quad (6)$$

where $K_{JT}^d(0)$ and $K^d(1)$ is the single-particle term evaluated using occupation numbers calculated with the Hamiltonian without \bar{P}_{JT} pairing and with the full Hamiltonian, respectively. This difference may give some idea about the change in the mixing with the high-lying j -shells as a result of pairing interaction, because particles occupying shells with large single-particle energy ε_j make larger influence to the total single-particle contribution, see eq.(5). (For example, change in the occupation of the $f_{5/2}$ shell by 0.1 particle and corresponding change in the $f_{7/2}$ shell occupation yields 0.6 MeV in ΔK^d , if the KB3 interaction is used.) In addition, it gives an idea of a fraction of the pairing energy coming due to single-particle contributions.

The difference ΔK_{JT}^d can be both positive and negative. If it is negative, more particles are excited to higher j -shells in the full calculation, while the pairing interaction (over)compensates the loss in the single particle contribution. If it is positive, the pairing interaction contributes to the gain of energy by favouring configuration with less particles excited from the lowest j -shells.

3 Results and discussion

It is known that the eigenfunctions of a well-bound states are less sensitive to a slight change of the potential, than the corresponding eigenvalues are. If two shell model Hamiltonians have two-body interaction being different by content of a pairing force, their eigenvalues are different but nuclear properties calculated using the corresponding eigenfunctions may be similar. The discussion of the role of pairing interaction is started from investigation of this interaction's influence on the nuclear wavefunction and quadrupole properties (subsection 3.1). It is known, that the pairing interaction does not affect quadrupole properties [28, 29]. It is, however, shown here that there are cases when this is not true. The influence of pairing interactions on energies is discussed afterwards, in subsection 3.2. A strict separation into these two topics cannot be made, thus the energies are also discussed together with wavefunctions.

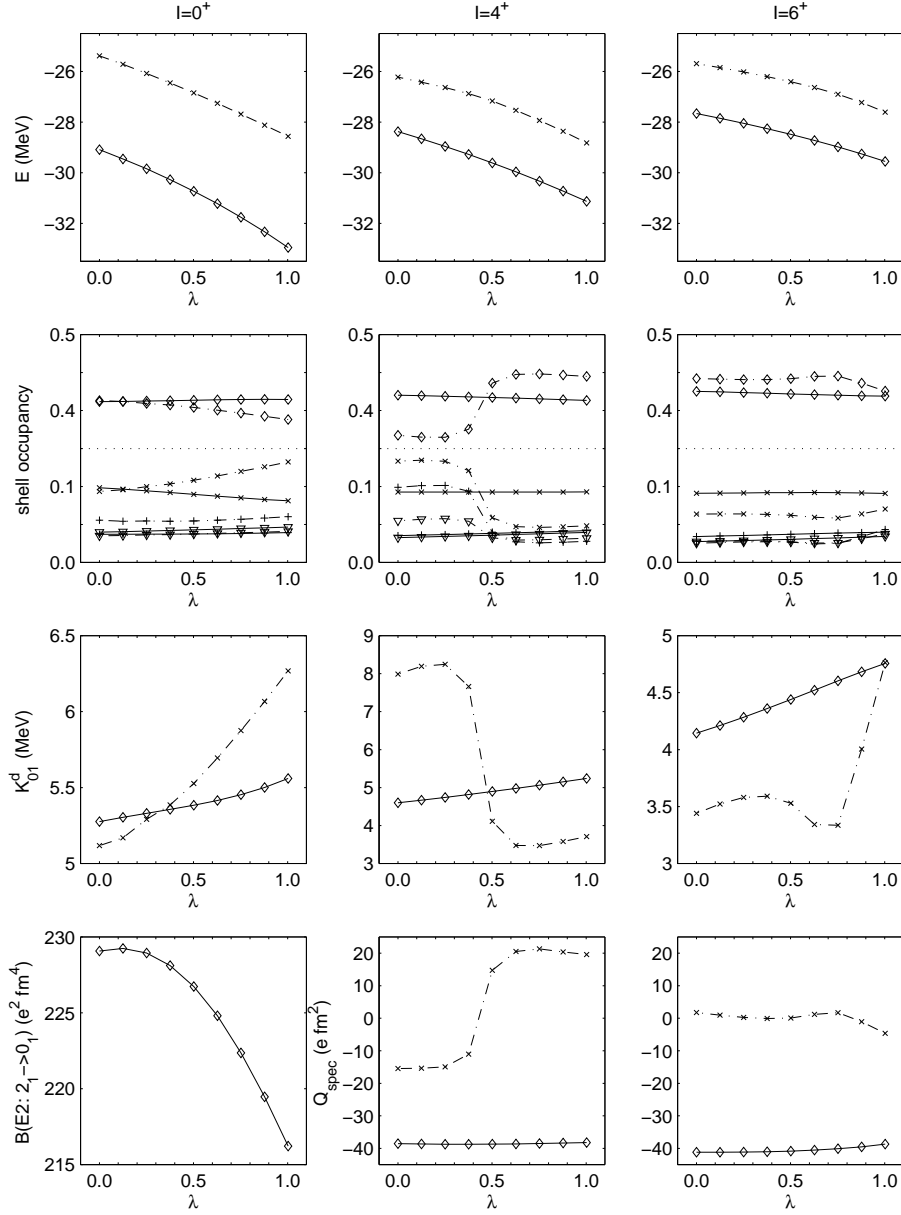


Figure 7: Energies, occupancies of the shells, single-particle contributions, and $E2$ properties of yrast and yrare states in ^{48}Cr calculated at spins $I^\pi=0^+, 4^+$ and 6^+ using the KB3 interaction. The \bar{P}_{01} pairing interaction content is given on the horizontal axis ($\lambda=0$ means no-pairing interaction, while $\lambda=1$ means full pairing interaction is present in the Hamiltonian). The top-row plots show the energies, E ; the second-row plots show shell occupancies; the third-row plots show the single-particle contributions, K_{01}^d ; and the bottom-row plots show $E2$ properties: $E2$ transition strength between yrast 2^+ and 0^+ states, and the spectroscopic quadrupole moment Q_{spec} at spins $I=4^+$ and 6^+ . The solid and dot-dashed lines are used to distinguish the yrast and yrare states, respectively. The $f_{7/2}$ shell occupancy is marked by diamonds, $p_{3/2}$ by crosses, $p_{1/2}$ by pluses, and $f_{5/2}$ by triangles.

3.1 Nuclear wavefunction and quadrupole properties

In general, the change in energy of a state $E_{JT}(\lambda; I)$ as pairing content (i.e. the λ value) increases, illustrates two effects. Besides a direct effect coming from the increased binding of certain nucleon pairs (linear in λ), there is an additional increase in energy (non-linear) due to the change of the number of such pairs that also results in abandoning of some less favourable configurations, i.e. the “structural effect” or χ in eq.(3). From fig.6 one may see that the structural effect increases the binding energy: if we start from the Hamiltonian without, say, \bar{P}_{01} pairing, there are not so many $JT=01$ coupled pairs, and the slope is not large. But as λ approaches 1, it becomes more and more favourable to form such pairs, and the $E(\lambda; I)$ curve bends down. If we start from the full Hamiltonian and reduce the amount of \bar{P}_{01} pairing, the energy loss would be much larger if the nuclear wave function is fixed than it is when configuration change is allowed.

Investigation of the pairing interaction effect on a particular state in a perturbative way may reveal a gradual change of the state properties. Changes are larger, when there is another close lying state, since these states may mix in a different proportion following the change of the interaction. As a result, when varying λ , one can see a mutual interchange of state properties. In an extreme situation, either sharp or gradual transition of the state properties from those of one state to those of the other state may be observed.

Let us first investigate a case, when there is a substantial energy distance between two states, thus other states do not influence the change of the state properties. The fig.7 shows some properties of the first and second excited states in ^{48}Cr calculated at spins $I=0, 4$ and 6^+ using the KB3 interaction, and the content of \bar{P}_{01} interaction is varied. Those properties are: state energy, j -shell occupation numbers, single-particle contribution to the total energy, and spectroscopic quadrupole moment Q_{spec} (or $E2$ transition strength where Q_{spec} is not defined). It is seen that the energy of the yrast states decreases (binding increases) as λ increases, but the occupancies almost do not change (except for the $p_{3/2}$ shell occupancy at 0^+). Some occupancies are difficult to distinguish in the plot, however, their values are not important for the discussion. The occupancies may be summarized in terms of the single particle contribution to the state energy, see eq.(5). As can be seen from the figure, K_{01}^{d} of the yrast states changes only slightly or not at all. One may also notice that the wavefunction of the yrare state at 0^+ is more affected by the change in pairing force than the yrast state (occupation numbers and thus K_{01}^{d} change more than in the yrast state). In addition, the second state at $I=4^+$ interacts with the third state, and the occupancies, the single-particle contribution as well as spectroscopic quadrupole moment change drastically at $\lambda \approx 0.45$, while the state energy only slightly changes slope. A similar change is seen at 6_2^+ .

The bottom-row plots in fig.7 show calculated $E2$ properties in ^{48}Cr as a function of \bar{P}_{01} pairing interaction content. As may be seen, the behaviour of the spectroscopic moment, Q_{spec} , is very similar to that of the single-particle contribution, K_{01}^{d} : if K_{01}^{d} does not change, the Q_{spec} does the same. However, it is wrong to correlate the increasing $f_{7/2}$ shell occupancy (K_{01}^{d} tends to 0) with the more oblate nuclear shape ($Q_{\text{spec}} > 0$). The “center-of-the-shell” rule (mentioned in subsection 2.2 above) demands $Q_{\text{spec}} = 0$ for $K^{\text{d}} = 0$, however, as can be seen from the figure, small admixtures of other j -shells causes deviation from the rule. The bottom-left plot shows the strength of the stretched $E2$ transition between the lowest yrast states, $2_1^+ \rightarrow 0_1^+$. As more pairing interaction is present in the Hamiltonian (λ increases), less particles are excited from the $f_{7/2}$ shell (K_{01}^{d} decreases), thus prolate nuclear deformation decreases (cf. the behaviour of K_{01}^{d} and Q_{spec} at $I=4_2^+$). This is in agreement with the “center-of-the-shell” rule. However, the low probability of pure $f_{7/2}^8$

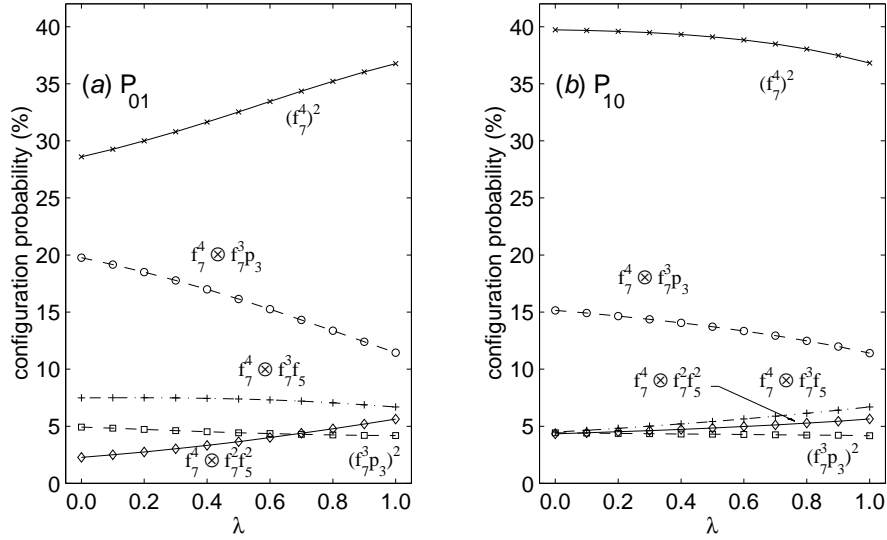


Figure 8: Calculated probabilities of configurations in the ^{48}Cr ground state as a function of \bar{P}_{JT} pairing interaction content, λ : the left and right plots show \bar{P}_{01} and \bar{P}_{10} cases, respectively. The KB3 interaction was used in the calculation. Only configurations with probability exceeding 5% at some point are shown. The missing probability is about 33%.

configuration (see below) as well as changing Q_{spec} of 2_1^+ state (not shown here) suggests that a bit more sophisticated picture than the mentioned selection rule is needed. Note, however, that the reduction of the $B(E2)$ value by 6% means only insignificant change in an approximate quadrupole deformation β_2 (calculated assuming the axially symmetric rotor model is valid): from $\beta_2=0.270$ to 0.263.

Although the binding energy of the yrast state changes significantly due to a change in the pairing interaction content, the occupation numbers change only slightly, and only a more detailed view of the probabilities of different configurations reveal changes. As an example, configurations in the ground state of ^{48}Cr are shown in fig.8. Those configurations which never achieved probability larger than 5% are omitted. The missing probability, i.e. summed probability of not shown configurations, constitutes 35% and 31-35% for \bar{P}_{01} and \bar{P}_{10} cases, respectively. The average numbers of particles in j -shells are unevenly distributed among the omitted configurations. For example, the missing particle numbers are 1.8 for $f_{7/2}$, 0.5 for $p_{3/2}$, 0.2 for $p_{1/2}$ and 0.4 for $f_{5/2}$ shell in the case of \bar{P}_{01} pairing interaction. The probabilities marked like $f_{7/2}^4 \otimes f_{7/2}^3 p_{3/2}$ are added probabilities of configurations $\pi f_{7/2}^4 \nu (f_{7/2}^3 p_{3/2})$ and $\pi (f_{7/2}^3 p_{3/2}) \nu f_{7/2}^4$ (here π stands for protons and ν for neutrons), while marks like $(f_{7/2}^4)^2$ indicate that protons and neutrons have the same configuration ($f_{7/2}^4$ in this example). The fig.8a shows that the probability of configurations where all 8 particles are in the $f_{7/2}$ shell is increasing by 8% in the \bar{P}_{01} case, when λ goes from 0 (no pairing) to 1 (full pairing). At the same time, the configurations with one particle excited to $p_{3/2}$ decreases by the same amount. The \bar{P}_{01} pairing increases the probability of configurations with two particles of the same kind being excited to $f_{5/2}$ by 3%, but this probability reaches only about 6% at the maximum. The mixing with $p_{3/2}$ may be favourable at $\lambda=0$, but at $\lambda=1$, where $JT=01$ pairs are more favoured in energy, shells with large ℓ , i.e. $f_{7/2}$ and $f_{5/2}$, are more important. The fig.8b shows that the \bar{P}_{10} interaction lowers the probability of $f_{7/2}^8$ as well as $f_{7/2}^7 p_{3/2}$ configurations by 4% each; while the probabilities of configurations with one or two particles in the $f_{5/2}$ shell slightly

increase.

Information about changes in the nuclear wavefunction are still hidden in fig.8: the linear change of configuration probabilities does not explain non-linear change of the state energy (see fig.6). It may be suspected that the average seniority changes in a nonlinear manner.

An example, where the two lowest-lying states affect each other when the pairing interaction content changes, may be taken from ^{90}Rh calculated using the SSSV interaction. Fig.9 illustrates three cases of the two interacting states calculated for the \bar{P}_{01} force: weak mutual influence at spin $I^\pi=13^+$, smooth “crossing” at 17^+ , and sharp crossing at 19^+ . The states hardly influence each other at spin $I=13^+$ (see left column plots in fig.9). Although the energy difference between the states remains approximately constant as more pairing is added (i.e., λ approaches 1), properties of the states change in a correlated way: in the yrast state the $g_{9/2}$ shell becomes more mixed with other j -shells, while the opposite is seen in the yrare state. This change in shell mixing can be seen both from the shell occupancies by particles and from the single-hole contribution, K_{01}^d . Note that the single-hole contribution in ^{90}Rh behaves in an opposite way than the single-particle contribution in ^{48}Cr when trend is compared to the occupation of the high- j shell: if the $f_{7/2}$ shell occupancy increases, cf. fig.7, the single-particle contribution in ^{48}Cr decreases, while the $g_{9/2}$ occupancy by particles and the single-hole contribution in ^{90}Rh increase or decrease together. The two lowest states come closer in energy and separate again at spin $I=17^+$ (see middle column plots in fig.9). The behaviour of occupation numbers (or of the single-hole contribution) suggests that the states gradually exchange their properties, since the shell occupancies of one state at $\lambda=0$ become equal to those of the other state at $\lambda=1$. A similar picture is seen at spin $I=19^+$ where the two states approach and cross each other without much interaction: the energy slope changes sharply at $\lambda=0.9$ and both the occupancies and thus the single-hole contributions change abruptly. In this case it is possible to calculate the pairing energy of a specific configuration, i.e. of the configuration being yrast at $\lambda=1$, or of the one being yrast at $\lambda=0$.

The bottom-row plots of fig.9 show Q_{spec} calculated in ^{90}Rh using the SSSV interaction for the three spin values discussed above. It is clearly seen that Q_{spec} is correlated with the single-hole contribution, K_{01}^d . For the less mixed configurations (small K_{01}^d values), Q_{spec} tends to zero; while for the more mixed configurations (larger K_{01}^d), the prolate deformation increases (Q_{spec} decreases). A picture of the mutual influence between the two states, obtained plotting the deformation coordinate (or Q_{spec} , assuming the axial symmetry) at horizontal axis and energy at vertical axis, would be somewhat different than the one described above. If the positions of points representing values of first and second states for a given spin are followed as λ goes from 0 to 1, one would see, that the “minima” are well separated by deformation, and they merely “sink” (i.e., the binding increases) at spin 13^+ . A bit more complicated picture occurs at spin 17^+ , where minima are separated for λ values close to the limits, but at $\lambda\approx 0.7$ the two states should be treated as first and second state in the same potential well and not as separate minima. The properties of states are also very similar there (see fig.9, middle column). At spin 19^+ , there minima are well separated by deformation for $\lambda=0$. But for larger λ values, the well depths increase at a different rate and become more and more similar. As a result, the wavefunctions start to mix, and finally, the state having larger deformation becomes yrast. A similar sharp transition between two states may occur in the backbending regions, if the crossing bands have different pairing properties.

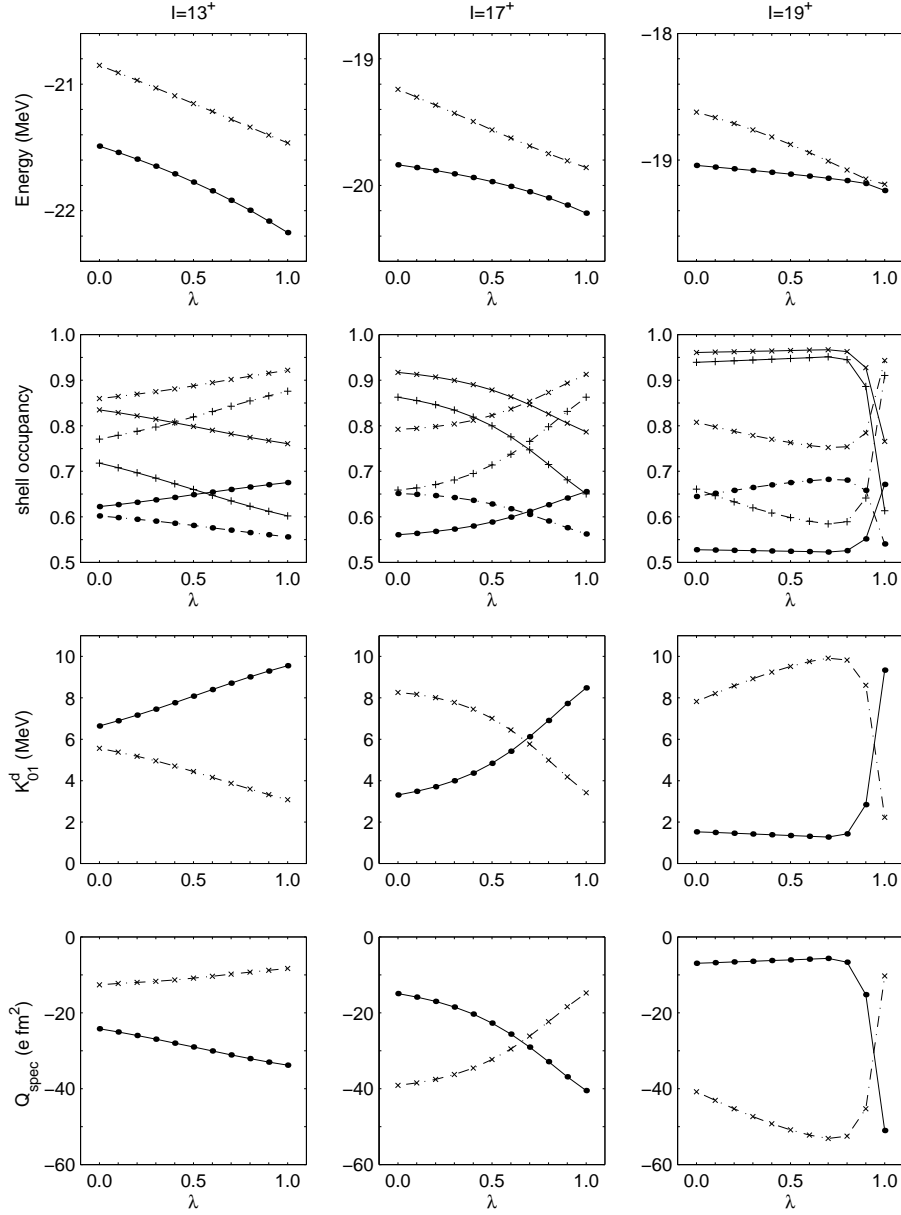


Figure 9: Some properties of yrast and yrare states in ^{90}Rh calculated at spins $I=13^+$, 17^+ and 19^+ , using the SSSV interaction, as a function of the \bar{P}_{01} pairing interaction content. For explanations see fig.7. The particle occupancy of the $g_{9/2}$ shell is shown by filled circles, $p_{3/2}$ by crosses, $p_{1/2}$ by pluses. The single-hole contribution K_{01}^d is shown in the third-row plots.

From the presented here cases of two interacting states one may see, that the ($JT=01$) pairing increases shell mixing and may unfavour the pure high- j shell configurations. Thus deviations from the single- j picture of the pairing energy spin dependence, discussed in subsection 2.1, may be expected. Although only the \bar{P}_{01} cases were discussed here, a similar picture is obtained when \bar{P}_{10} interaction content is varied.

3.2 State energy

In the previous subsection it was already discussed that the increase of pairing interaction content yields additional binding of the state. This subsection discusses changes in the binding energy of yrast states. First of all, investigation of the obtained pairing energy dependence on the model space is presented. Then pairing energy dependence on the residual interaction is briefly reviewed. And finally, the pairing energy in the selected bands is discussed.

3.2.1 Model space effects

During discussion of the role of pairing interactions, a natural question may be asked, whether the model space is sufficient to trust the results. For example, the definition of schematic pairing forces ($L=0$) suggests that it is important to include both the high- j shell and its spin-orbit partner in the model space, in order to get reasonable pairing energy values. Thus the model space for ^{90}Rh is probably too small, since the $g_{7/2}$ shell is excluded. This section tries to shed some light on this problem.

To investigate the question whether the pairing energy, defined by eq.(4), is model space independent, yrast states of ^{48}Cr were calculated in different model spaces made of different combinations of j -shells from the pf major shell but using the same residual interaction, KB3. Experimental energies of the yrast states are reproduced with a different success in the selected model spaces, but in this investigation only the response to the change of pairing interaction content is important. The derived pairing energies (defined as energy difference between yrast states calculated with the Hamiltonian having no \bar{P}_{JT} pairing interaction and with the full Hamiltonian) are shown in fig.10: \bar{P}_{01} case is shown on the left, and \bar{P}_{10} case is shown on the right. It may be seen that the largest contribution comes from the spin-orbit partners having large orbital angular momentum ℓ . Thus the change in binding energies calculated in the full pf model space is almost completely accounted for in a smaller model space containing both $f_{7/2}$ and $f_{5/2}$. It is somewhat surprising that there are no obvious signs of a model space increase from $f_{7/2}f_{5/2}$ to full pf for both \bar{P}_{01} and \bar{P}_{10} forces. This may be understood taking into account the relatively small orbital angular momentum of the $p_{3/2}$ and $p_{1/2}$ shells, as well as from small occupancies of the j -shells other than the high- j shell (see fig.7 and ref.[14]).

The similarity of the pairing energy in the $f_{7/2}f_{5/2}$ and full pf calculations suggests that there is some saturation of the pairing interaction influence, and the change in nucleus structure accounts for the interaction change. That is also suggested by the model space dependence of the change in the single particle contributions (see below).

One conclusion which could be drawn from this investigation is that the approximate energy change due to the \bar{P}_{01} force as a function of spin can be obtained from the calculation in a model space without the spin-orbit partner, for example, $f_{7/2}p_{3/2}$ or $f_{7/2}p_{3/2}p_{1/2}$ (see fig.10a). The absolute magnitude can be estimated multiplying the pairing energy obtained in a more restricted model space by the ratio of model space degeneracies. For example, if one takes the result of the $f_{7/2}p_{3/2}p_{1/2}$ model space and multiplies it by 20/14, the estimated ΔE_{01} for the full pf calculation is only slightly too large: the difference is about 0.3 MeV for spins $I=0$ and 2^+ and less for other spin values. However, the predicted slope between states having spins $I=8$ and 10 is different from that in the full calculation. Such scaling does not work for the \bar{P}_{10} force (see fig.10b), where inclusion of $f_{5/2}$ is necessary to obtain the profile of the ΔE_{10} spin-dependence. One may also notice, that the inclusion of the $f_{5/2}$ shell into the model space approximately doubled

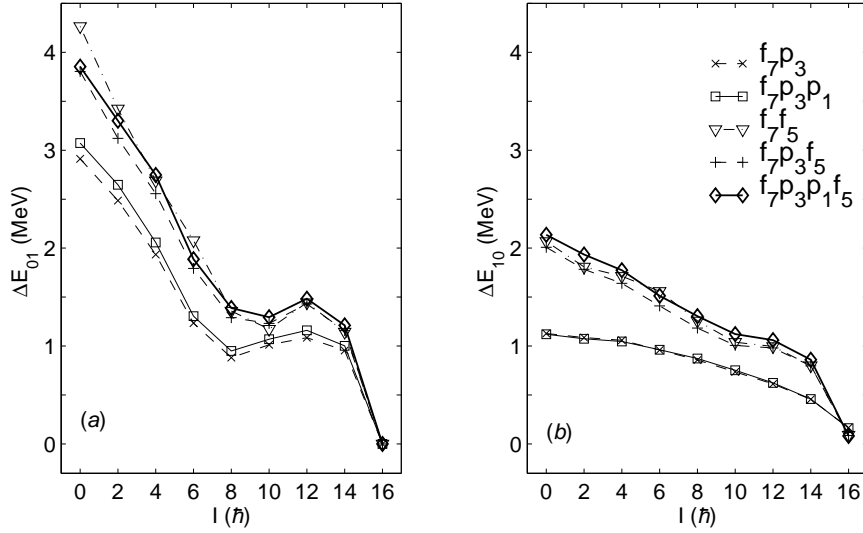


Figure 10: Model space dependence of the pairing energy. Calculated for the ^{48}Cr nucleus using KB3 interaction. The left (right) plot shows \bar{P}_{01} (\bar{P}_{10}) case.

the calculated \bar{P}_{10} pairing energy.

This investigation, however, leaves the question, whether inclusion of the other major shells would change the pairing energy. One would expect that the influence of higher lying j -shells is not large because a large difference in single-particle energies would limit the mixing. If, however, the shells below the lowest partially-filled shell (the “lower shells”) are included in the model space, the pairing interaction effect should be separated into a part coming from the lower shells and the rest, because the lower shells always react to the change of the pairing interaction content (since they are mostly filled).

The model space dependence of a difference in the single-particle contribution, ΔK_{JT}^d , defined by eq.(6), is shown in fig.11. This difference gives some idea about the change in the mixing with the high-lying j -shells as a result of pairing interaction. It can be seen that ΔK_{JT}^d behaves in a rather irregular way, as compared to the total change in energy (fig.10), and it is not possible to predict how the contribution will change with an increase of the model space. However, there are also similarities in the change of the single-particle contributions. For example, it is clearly seen, that the pairing interactions favour configurations with more particles excited to higher shells in the model spaces containing both $f_{7/2}$ and $f_{5/2}$ shells (except for $I=0^+$ and 12^+ states calculated for the \bar{P}_{01} case in the full pf model space), since $\Delta K_{JT}^d < 0$. The opposite is seen for most spin values in the $f_{7/2}p_{3/2}$ \bar{P}_{01} case. It is also interesting to note that the \bar{P}_{10} force decreases shell mixing at the maximum spin state $I_m=16^+$, since ΔK_{JT}^d is positive here.

In summary, the investigation of the model space dependence of the pairing energy suggests that the model space containing shells slightly above the lowest partially-filled shell is sufficient to investigate the influence of the \bar{P}_{01} pairing interaction on the state energies, while the \bar{P}_{10} pairing energy can be obtained only in model spaces containing both the high- j shell and its spin-orbit partner.

3.2.2 Residual interaction dependence

Somewhat different investigation is the calculation of energy changes in the same nucleus using different interactions. If the residual force is unique, the difference in the calculated

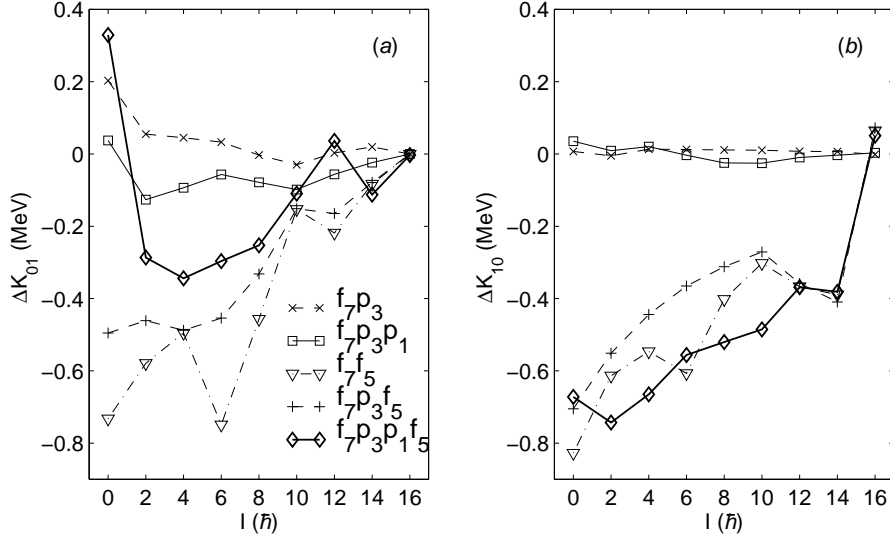


Figure 11: Model space dependence of the difference in single-particle contribution, $\Delta K_{JT}^d = K_{JT}^d(0) - K_{JT}^d(1)$. Calculated for nucleus ^{48}Cr using the KB3 interaction. The left (right) plot shows \bar{P}_{01} (\bar{P}_{10}) case.

pairing energy would come only from the model space difference. However, since there is no unique force yet, the agreement in the pairing energy, if occurs, is more likely to be accidental, and there should be clear dependence on the chosen residual interaction. A separate question is whether this dependence should show up *only* as different nonlinear effects, χ in eq.(3). If the nuclear mean-field (Hartree-Fock field) is universal (cf. discussion about the universal multipole part of the Hamiltonian in ref.[7], that gave foundation for this investigation), one would expect that the average number of pairs in the wavefunction calculated using the Hamiltonian without pairing interaction is independent on the chosen (full) residual interaction. A disagreement in this average number of pairs would come from the other multipole terms favouring certain two-nucleon states, different in different residual interactions. The average number of pairs is proportional to $\langle W_{JT} \rangle$ in eq.(3), thus more information will be provided in the subsection 3.2.3, when the coefficients of the state energy decomposition, eq.(3), will be presented.

The investigation was performed for ^{90}Rh using GF and SLGT0 interactions in the configuration space $(p_{1/2}g_{9/2})^{14}$, as well as the SSSV interaction in $(g_{9/2}p_{1/2}p_{3/2})^{-10}$. The calculated pairing energies are shown in fig.12. To take into account the effect of the lower shells (in our case, of the $p_{1/2}$ shell), which was discussed in subsection 3.2.1, pairing energy calculated in ^{90}Rh using GF and SLGT0 interactions was approximately corrected taking the maximum spin state $I_m=25^+$ as a reference. There spin is produced by 10 particles in $g_{9/2}$ shell, and the $p_{1/2}$ shell is full. There is no non-linear dependence on the pairing interaction content, i.e. $\chi(\lambda) \equiv 0$ at this state. Thus the values obtained in the GF and SLGT0 calculations are shifted down to match the SSSV value at the maximum spin state $I_m=25^+$. GF pairing energies are reduced by 0.66 and 0.24 MeV for \bar{P}_{01} and \bar{P}_{10} cases respectively. The corresponding values for the SLGT0 interaction are 0.80 and 0.12 MeV. As explained in the subsection 3.1 above, due to a sharp “crossing” in the energies $E_{JT}(\lambda; I)$ calculated with the SSSV interaction, it is possible to calculate the pairing energy of configurations becoming yrast in the full Hamiltonian and being yrare in the Hamiltonian without pairing. These values, $E_2(0) - E_1(1)$ (here subscript refers to the state number for a given spin and total isospin), calculated at spins $I=15^+$ and 19^+ are

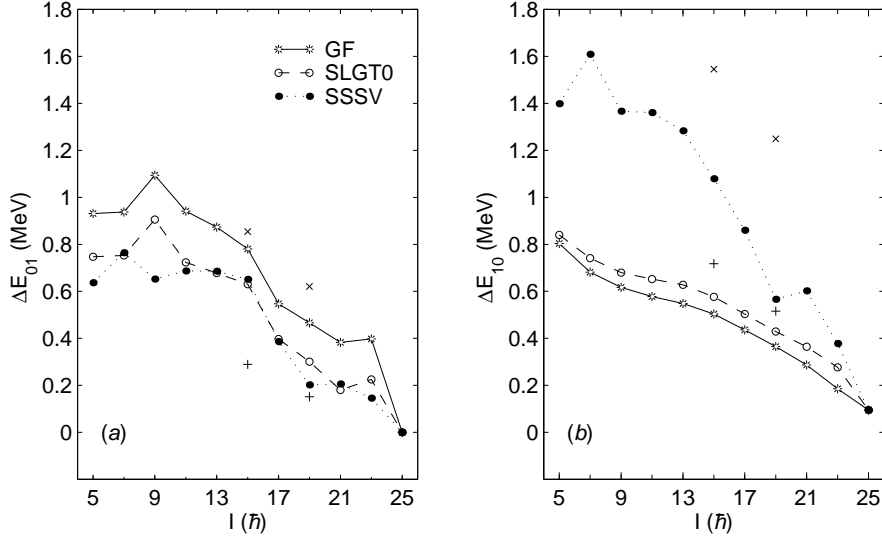


Figure 12: Interaction dependence of the pairing energy calculated for ^{90}Rh nucleus using three interactions. The left (right) plot shows \bar{P}_{01} (\bar{P}_{10}) case. The GF and SLGT0 values are shifted down to match the SSSV value at spin $I=25^+$. For spins $I=15^+$ and 19^+ , the SSSV energy differences between yrare at $\lambda=0$ and yrast at $\lambda=1$ states are indicated by cross signs, and the energy differences between states behaving in an opposite way are marked by plus signs.

marked by crosses in the fig.12. The pairing energy of configurations which become yrare in the full Hamiltonian, $E_1(0)-E_2(1)$, are shown by pluses. The figure clearly shows that the configuration becoming yrast in the calculation with the full interaction gets much more pairing energy than the yrare configuration.

As seen from the figure 12a, the spin dependence of \bar{P}_{01} pairing energies, obtained from different interactions, is very similar, especially between the GF and SLGT0 interactions calculated using the same model space. However, the absolute magnitude of pairing energy is different. The difference in the calculated \bar{P}_{01} pairing energies using GF and SSSV interactions cannot be explained by the model space effects (cf. fig.10): ΔE_{01} from the SSSV calculation should be larger than values obtained from the GF calculation. Thus it is the expected dependence on the residual interaction.

The origin of the difference in the spin dependence of \bar{P}_{01} pairing energy close to the band termination is not clear: in the SSSV case, there is a small increase in pairing energy at spin 21^+ (in a similar way as in ^{48}Cr at $I_m-4=12$, see fig.10), while in more restricted calculations using GF and SLGT0 interactions, the \bar{P}_{01} pairing energy is locally smaller at 21^+ and increases at $I=23^+$.

The above discussion of the model space effects (subsection 3.2.1) suggested, that the calculated \bar{P}_{10} pairing energies should be smooth if model space does not contain the spin-orbit partner of the high- j shell. And indeed, the ΔE_{10} values calculated for ^{90}Rh with GF and SLGT0 interactions are smooth (see fig.12b), like in model spaces without $f_{5/2}$ shell for ^{48}Cr , see fig.10. The SSSV calculated energies behave in a different way, suggesting the anticipated interaction dependence of the calculated pairing energy.

There are more cases when different interactions predict similar pairing energy. For example, the \bar{P}_{01} pairing energy calculated along the ground state band in ^{48}Cr using the modified surface-delta interaction in the model space ($f_{7/2}p_{1/2}$) [12] is very similar to the values calculated using the KB3 interaction in the full pf model space. In addition, even

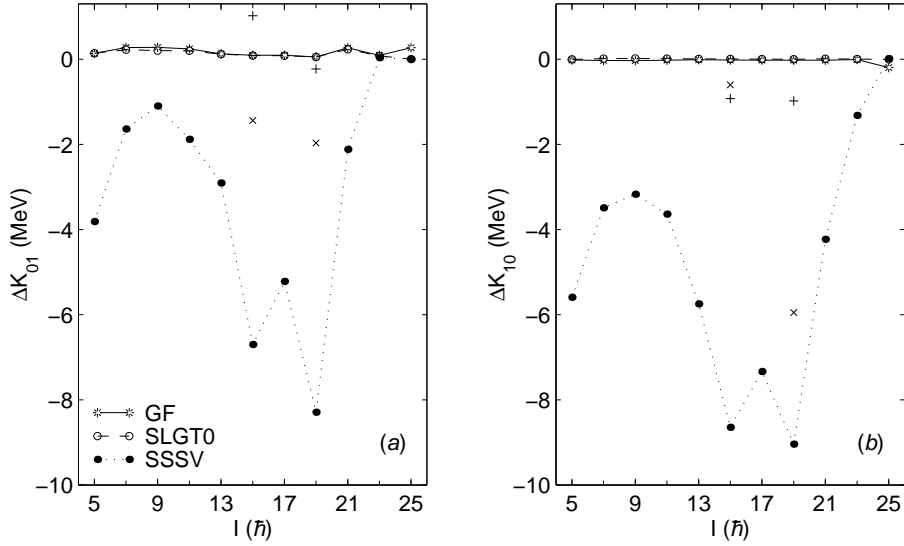


Figure 13: Interaction dependence of the single-particle contribution difference calculated for ^{90}Rh nucleus using GF, SLGT0 and SSSV interactions. In the latter case the single-hole contribution difference is shown. The left (right) plot shows \bar{P}_{01} (\bar{P}_{10}) case. The notation is the same as in fig.12.

the decomposition into direct and structural effects (eq.(3)) gives almost identical values. The MSDI parameters were fitted to reproduce experimental energies in this nucleus, thus the model space effect, i.e. the absence of $f_{5/2}$, was probably remedied by this adjustment. The \bar{P}_{10} pairing energy calculated with MSDI is smaller than the one obtained using KB3 in the same model space, shown in fig.10.

Fitting to the energies, in general, does not imply that all energy-related properties will be well described. For example, the \bar{P}_{01} pairing energy, calculated for ^{48}Cr using the surface-delta interaction fitted to the energies in the full pf model space (the parameter values $A_T=0.2+0.4T$), is larger than KB3 values. However, the spin dependence has the same profile.

The single-particle contribution difference, calculated in ^{90}Rh using three different residual interactions, is shown in fig.13. As was already seen from the model space investigation of ΔK^d , the contributions may be different in these calculations, first of all, because of the different model spaces. Thus the K^d values obtained in GF and SLGT0 interactions, being one similar to another, should be expected to be different from the the SSSV values. As seen from the figure, the pairing interactions favour configurations with more holes excited from the $g_{9/2}$ shell in the SSSV calculation. A similar conclusion was made for ^{48}Cr .

3.2.3 Pairing energy

The JT pairing energies, calculated for three selected nuclei, are shown in fig.14. The spin values in ^{22}Na and ^{48}Cr calculations are shifted to match the maximum spin value $I_m=25^+$ of the selected band in ^{90}Rh by 16 and $9\hbar$, respectively. Pairing energies in ^{22}Na and ^{48}Cr are shown as obtained from the calculations using USD and KB3 interactions, respectively. While for the nucleus ^{90}Rh , the estimated \bar{P}_{01} pairing energy is shown. Estimation tries to account for the spin-orbit partner of the $g_{9/2}$ shell, namely the $g_{7/2}$ shell, that is not included in the model space. It is made by assuming that the pairing energy scales with

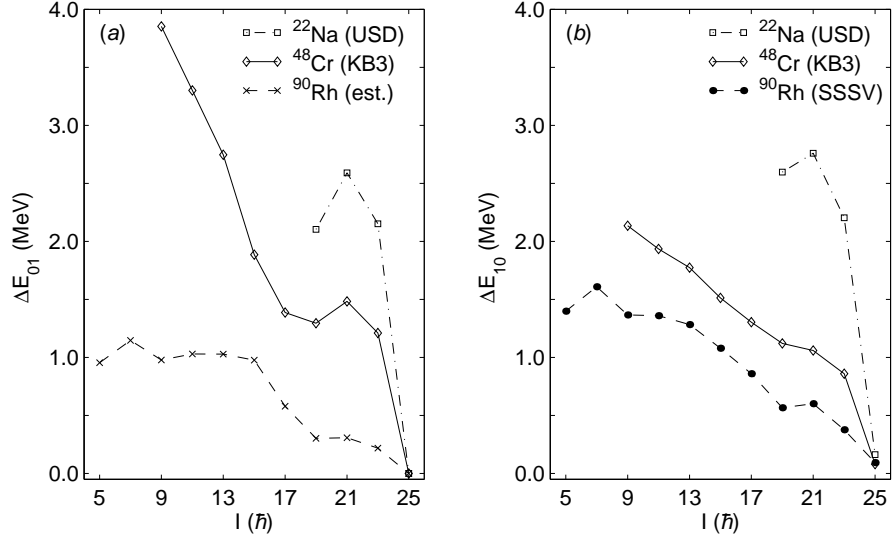


Figure 14: Spin dependence of the calculated pairing energy in the selected bands of ^{22}Na , ^{48}Cr and ^{90}Rh nuclei. For explanations see text. The \bar{P}_{01} (\bar{P}_{10}) case is shown on the left (right).

the model space degeneracy, as suggested by the model space investigation in subsection 3.2.1. The estimation is based on the calculated SSSV pairing energies (since they are obtained in a larger model space than, say, GF values), thus the scaling parameter is 1.5. The \bar{P}_{10} pairing energy in ^{90}Rh is taken as obtained using the SSSV interaction, because \bar{P}_{10} energies do not scale with the model space. As can be seen from the figure, both the \bar{P}_{01} and \bar{P}_{10} pairing energies decrease as spin increases (on the average). In addition, the values are similar in magnitude for the odd-odd nuclei, ^{22}Na and ^{90}Rh . In the ^{90}Rh calculation using the SSSV interaction ΔE_{10} is even larger than ΔE_{01} . While in the case of even-even nucleus, ^{48}Cr , the influence of $JT=01$ interaction is larger, as was also shown in ref.[8]. Thus both pairing interactions reduce the moment of inertia. However, the relative importance of \bar{P}_{01} and \bar{P}_{10} pairings to the moment of inertia in $N=Z$ nuclei depends on whether it is an odd-odd or even-even nucleus; in addition, it depends on the total isospin of states as well as on the oddity of state spin. Fig.14 shows that the spin dependencies of \bar{P}_{01} and \bar{P}_{10} pairing energies are more or less correlated. Those issues are addressed in a greater detail in ref.[11] where pairing properties of the rotational bands in the odd-odd $N=Z$ nucleus ^{62}Ga are discussed.

Due to a spin shift when plotting, it is easier to see that the irregularities in the spin dependence of the \bar{P}_{01} pairing energies are similar in the bands (see fig.14a). There is no $JT=01$ coupled pairs in the aligned, band terminating state, thus there is no pairing energy at spin I_m . There is a local maximum at spin I_m-4 , which happens to be the backbending point in ^{48}Cr and ^{90}Rh (see figs. 2 and 3). This state was also described as the maximum spin state for seniority $v_{\text{max}}-4$ (where $v_{\text{max}}=2j+1$), and the discussion in subsection 2.1 suggests that the pairing energy should be smaller in the neighbouring states: at higher spins the total seniority becomes larger; while at spin I_m-6 seniority is the same as in state I_m-4 in a single- j picture, however, this state is less resistant to the shell mixing that breaks $JT=01$ pairs, since it is not “maximum spin for a given seniority” state [12]. The \bar{P}_{01} pairing energy increases as spin decreases from I_m-6 to I_m-10 , and continues to increase for ^{48}Cr towards the lower spins, but remains rather constant for ^{90}Rh . It may be an effect from the $T=1$ pairing blocking in $T_{\text{tot}}=0$ states of an odd-odd

nucleus.

The spin shift reveals also similarities of the ΔE_{10} spin-behaviour when values are compared starting from the band terminating state, see fig.14*b*. The I_m-4 state has an irregularity as compared with the trend of lower spin states. For the spins below I_m-4 , the ΔE_{10} is almost a linear function of spin. In ^{48}Cr there is a slight increase of ΔE_{10} (as compared with this linear interpolation) at spin $I_m-12=4^+$. This spin value is the lowest state if only \bar{P}_{10} pairing interaction constitutes the complete interaction. Thus it may be a signature, that KB3 contains overestimated \bar{P}_{10} force (cf. fig.1), because a similar irregularity is also seen in the full energy spectrum with a rotational reference subtracted, while there is no such irregularity in experimental data (see fig.2).

The parameter values in the decomposition of \bar{P}_{JT} pairing energies, see eqs.(3) and (4), are shown in fig.15: plots in the top row show expectation values of the normalized pairing interaction $\langle W_{JT} \rangle$, while the bottom row plots show the total structural effect $\chi_{JT}(1)$. Like in fig.14, the spin values for ^{22}Na and ^{48}Cr are shifted. The parameter values for ^{22}Na and ^{48}Cr are calculated using USD and KB3 interactions, respectively. For the ^{90}Rh nucleus, parameter values obtained using all three interactions, GF, SLGT0 as well as SSSV, are given. The values are not scaled to estimate the effect from the excluded $g_{7/2}$ shell. The irregularities of $\chi(1)$ values calculated for ^{90}Rh may be attributed to the two state interaction, discussed in section 3.1. To eliminate the effect coming from particles in the $p_{1/2}$ shell, the $\langle W_{JT} \rangle$ values obtained in the GF as well as SLGT0 calculations are shifted down to match the SSSV value at $I=25^+$ (cf. fig.12). The $\chi(1)$ values show that the non-linear term, and thus the reconfiguration effect, is not negligible and plays an important role in shaping the spin dependence of the bands. In particular, there is an increase in the nonlinear contribution at spin $(I_m-4)\hbar$. The difference in the magnitude of the parameter values in ^{22}Na , ^{48}Cr and ^{90}Rh cannot be explained by simple mass scaling, $\hbar\omega$. There are additional effects, that may have origin in the dependence on the residual interaction.

As seen from the fig.15*a*, the expectation value of the \bar{P}_{01} interaction is approximately constant for spins ranging from I_m-2 to I_m-6 (or even I_m-8), suggesting that the average number of $JT=01$ pairs in this spin range is not changing in the Hamiltonian without \bar{P}_{01} pairing interaction. The fig.15*c* suggests, that the structural effect is responsible for the increase of the pairing energy at spin I_m-4 . The figs.15*a* and *c* suggest, that the unfavoured band termination is due to the equal number of $JT=01$ pairs at spins $I=I_m-4$ and I_m-2 in the calculation without this pairing interaction, since the structural effect changes by the same amount when going from I_m-4 to I_m-2 , and finally I_m state. The $T=0$ pairing helps in making the I_m state unfavourable: here the change in the pairing energy is larger when going from I_m-2 to I_m state as compared to the change between states I_m-4 and I_m-2 .

The structural change is also important for the effect coming from the \bar{P}_{10} interaction (see plots in the right-column of fig.15). The expectation value of the pairing interaction has smoother spin dependence than the pairing energy does in the odd-odd nuclei (cf. fig.14). It is interesting to note, that the difference in ΔE_{10} between the GF (or SLGT0) and SSSV interactions is coming from the structural effects, while the average number of $L=0$, $S=J=1$, $T=0$ pairs is the same at $\lambda=0$.

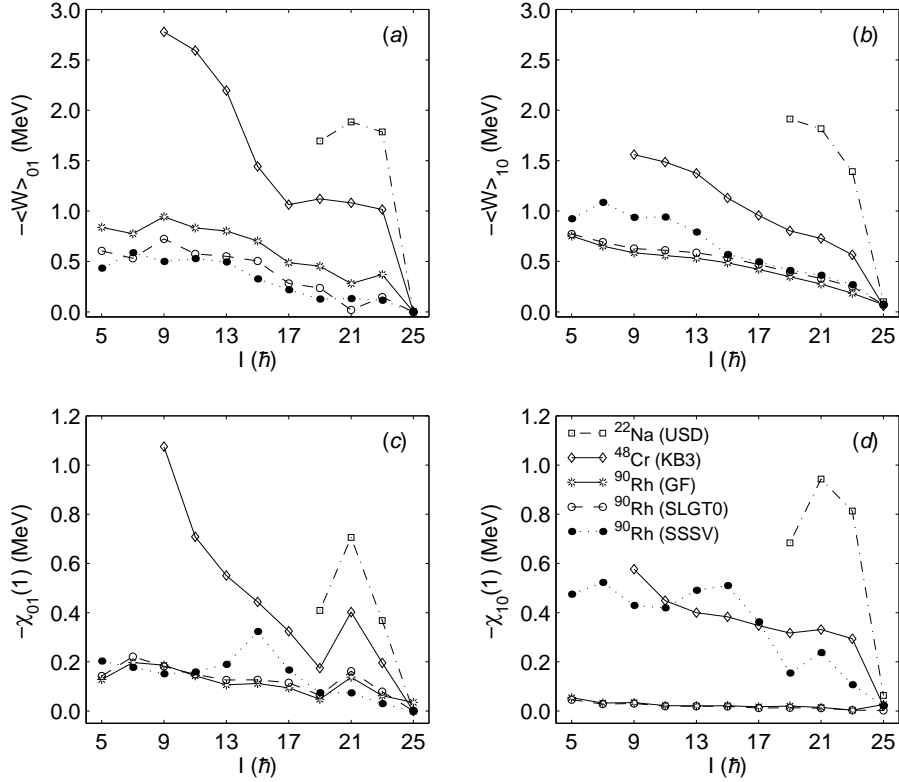


Figure 15: Parameterization coefficients of the pairing energy, see eqs.(3) and (4). Details are given in text. The left (right) column shows \bar{P}_{01} (\bar{P}_{10}) case.

4 Summary and conclusions

There are several ambiguities, when discussing the role of the pairing interaction in the shell model. First problem is the “no-pairing” Hamiltonian. Since it is defined as a deviation from the full Hamiltonian (see eq.(1)), the correctness of defining the magnitude of this deviation (i.e. the pairing strength) is crucial to have a correct Hamiltonian without pairing. Having selected (or fixed from other considerations) the strength of the pairing interactions, a question may be asked whether a *full* force is present in a chosen residual interaction. This question was also discussed in ref.[7], where it was argued that the multipole part of realistic interaction, that is responsible for particle correlations, including pairing interactions, is almost the same. Thus only small deviations from the pairing interaction content, estimated in this reference, are expected. However, the model space dependence of the pairing properties may yield unwanted effects.

Another problem is the form of the pairing interaction. The normalized $JT=01$ pairing interaction was shown [7] to remedy the divergence in the pairing plus quadrupole model, in the case when many shells are included in the model space. However, this normalized form still does not solve the divergence problem completely. Thus the form of the force is not final yet, and details of the derived role of pairing interactions may change.

The third problem is the interpretation of the role of a pairing interaction in comparison with that derived from other models. The difference in treatment of pairing correlations in the shell model and, say, Hartree-Fock-Bogolyubov approach puts a question whether comparison is meaningful.

The fourth problem is the relation between the pairing properties obtained in the shell

model and observables.

Having the above ambiguities in mind, let's summarize the presented investigation of the role of pairing interactions. Three selected bands in ^{22}Na , ^{48}Cr and ^{90}Rh , having the total isospin $T_{\text{tot}}=0$, were discussed. Their choice, based on the behaviour of the $JT=01$ pairing energy in a single- j shell model, was explained. Since there is no experimental data on ^{90}Rh available, three interactions were used to calculate its properties, and a comparison of their results was presented. All three interactions predict that the ground state is $I=0$, $T_{\text{tot}}=1$, and that the excitation energy to the lowest $T_{\text{tot}}=0$ states is approximately 1.3 MeV. In addition, the $K^\pi=5^+$ ($T_{\text{tot}}=0$) band, which was of interest in the present investigation, backbends at spin $I=19^+$. In the SSSV calculation, the backbending is related to a bandcrossing. The SSSV calculation should describe quadrupole properties more reliable, thus odd- I members of the $K=5^+$ band are expected to have a prolate deformation. The comparison of the energies calculated in ^{90}Rh using the GF (or SLGT0) and SSSV interactions raises a question, whether the model space used to describe ^{48}Cr yrast band is large enough to discuss also the high spin states. This question is supported by the observation that the deviation between calculated and observed energies is increasing after $I=10$ towards the aligned state at 16^+ (see fig.2). In addition, the proposed shell model explanation for the backbending as a result of interplay between the monopole and quadrupole forces [28] does not exclude the picture of the unpaired band-crossing (ground state band crosses with the $K^\pi=8^+$ band).

A perturbative approach to investigate the role of schematic normalized $L=0$ pairing interactions [7] was presented. Both $T=0$ and $T=1$ pairing interactions reduce the moment of inertia (that is in agreement with [8]), however their relative importance have interesting dependence on the spin oddity and total isospin of the states (see [11]). It was shown that the pairing force brings energy in two ways: (i) directly, due to an extra binding of certain pairs of nucleons, and (ii) indirectly, due to an increased likelihood to form those pairs. From the calculations it follows, that the indirect effect is as important as the direct effect.

Problems occurring during investigation of the role of pairing interactions were discussed. In particular, the case of two close-lying states was described. It was shown that the pairing interaction do not alter quadrupole properties, if the energy distance between the states is large enough.

The dependence of the pairing energy (the difference between energies of yrast states calculated from the Hamiltonian without pairing interaction and the full Hamiltonian) on the model space was investigated taking ^{48}Cr nucleus as an example. It was shown that the spin dependence of the \bar{P}_{01} pairing energy derived in the full model space may be estimated from the calculation in a smaller model space by taking into account the increased degeneracy of the model space. This observation was used to estimate the $JT=01$ pairing energy in ^{90}Rh as would be obtained if the $g_{7/2}$ shell would be included in the model space. It was also shown that the \bar{P}_{10} pairing energy does not scale with the model space degeneracy. The pairing energy dependence on the choice of the residual interaction was also discussed. During the investigations of those two dependencies, it was shown that the pairing interactions in most cases facilitate the shell mixing (a similar picture occurs in the BCS model).

The pairing energies calculated in the three selected bands were compared. It was shown, that if the spin values are shifted so that the aligned state having spin $I_m=(p+1)^2$ coincides, the spin dependencies of pairing energies in the three selected bands have similar profiles. The decomposition of the pairing energy into direct and indirect parts, available

due to a perturbative way of investigation, was also presented. It was shown that the similarities in the spin dependence of the coefficients remain.

Despite being rather detailed, this investigation raised questions which could not be answered. For example, the energy spectrum of ^{90}Rh remains an open question. The three used interactions predict different not only excitation energies, but also the energy distance between the yrast and yrare states. The origin of the backbend of the $K^\pi=5^+$ band in this nucleus is also unclear: whether it is similar to the one discussed in ref.[28] or it is “usual” backbending originating from a band-crossing. The investigation of the pairing energy dependence on the model space suggests that the calculation performed in the model space containing also $g_{7/2}$ shell may give somewhat different results than discussed here. The experimental data would provide a stringent test for the choice of the residual interaction.

In addition, a systematic study of the pairing energy dependence on the total isospin and the oddity of state spin is needed to add an understanding what is the origin of blocking effects.

Acknowledgments

The author thanks E. Caurier for access to the shell model code [15], and S. Åberg for useful discussions as well as comments on the manuscript. The financial support from The Swedish Institute (“The Visby Programme”) is also acknowledged.

References

- [1] G. Martínez-Pinedo, K. Langanke and P. Vogel, Nucl. Phys. A 651 (1999) 379.
- [2] A.L. Goodman, Adv. Nucl. Phys. 11 (1979) 263.
- [3] O. Civitarese, M. Reboiro, P. Vogel, Phys. Rev. C 56 (1997) 1849.
- [4] J. Terasaki, R. Wyss and P.-H. Heenen, Phys. Lett. B 437 (1998) 1.
- [5] A.L. Goodman, Phys. Rev. C60 (1999) 014311.
- [6] D.R. Bes and R.A. Sorensen, Adv. Nucl. Phys. 2 (1969) 129.
- [7] M. Dufour and A.P. Zuker, Phys. Rev. C 54 (1996) 1641.
- [8] A. Poves and G. Martínez-Pinedo, Phys. Lett. B 430 (1998) 203
- [9] S.M. Lenzi, Talk at the Crete conference, 1999; to be publ. in the conference proceedings in Phys.Scr.
- [10] S.M. Vincent, P.H. Regan, D.D. Warner, R.A. Bark, D. Blumenthal, M.P. Carpenter, C.N. Davids, W. Gelletly, R.V.F. Janssens, C.D. O’Leary, C.J. Lister, J. Simpson, D. Seweryniak, T. Saitoh, J. Schwartz, S. Törmänen, O. Juillet, F. Nowacki, P. Van Isacker, Phys.Lett. B 437 (1998) 264.
- [11] A. Juodagalvis and S. Åberg, to be submitted to Nucl. Phys.
- [12] A. Juodagalvis and S. Åberg, Phys. Lett. B 428 (1998) 227.

- [13] A. de Shalit and I. Talmi, Nuclear Shell Theory, Academic Press, 1963, p.433.
- [14] E. Caurier, J.L. Egido, G. Martínez-Pinedo, A. Poves, J. Retamosa, L.M. Robledo, and A.P. Zuker, Phys. Rev. Lett. 75 (1995) 2466.
- [15] E. Caurier, computer code ANTOINE, Strasbourg (1990).
- [16] B.H. Wildenthal, Prog. Part. Nucl. Phys. 11 (1984) 5.
- [17] A. Poves and A.P. Zuker, Phys. Rep. 70 (1981) 235.
- [18] R. Gross and A. Frenkel, Nucl. Phys. A267 (1976) 85.
- [19] H. Herndl and B.A. Brown, Nucl. Phys. A 627 (1997) 35.
- [20] J. Sinatkas, L.D. Skouras, D. Strottman, and J.D. Vergados, J. Phys. G 18 (1992) 1377, 1401.
- [21] W.J. Vermeer, D.M. Pringle, E.F. Garman, and I.F. Wright, Phys. Lett. B 217 (1989) 28.
- [22] F. Brandolini, S.M. Lenzi, D.R. Napoli, R.V. Ribas, H. Somacal, C.A. Ur, D. Bazzacco, J.A. Cameron, G. de Angelis, M. De Poli, C. Fahlander, A. Gadea, S. Lunardi, G. Martínez-Pinedo, N.H. Medina, C. Rossi Alvarez, J. Sánchez-Solano, C.E. Svensson, Nucl. Phys. A642 (1998) 387.
- [23] A.V. Afanasjev, D.B. Fossan, G.J. Lane and I. Ragnarsson, Phys. Rep. 322 (1999) 1.
- [24] E. Caurier, A.P. Zuker, A. Poves and G. Martínez-Pinedo, Phys. Rev. C 50 (1994) 225.
- [25] D. Dean, S. Koonin, K. Langanke and P.B. Radha, Phys. Lett. B 399 (1997) 1.
- [26] R.D. Lawson, Theory of the nuclear shell model, Clarendon Press, Oxford, 1980.
- [27] J. Duflo and A.P. Zuker, Phys. Rev. C 59 (1999) R2347.
- [28] A.P. Zuker, J. Retamosa, A. Poves, and E. Caurier, Phys. Rev. C 52 (1995) R1741.
- [29] A. Poves, J. Phys. G 25 (1999) 589.